Research Article

On the Evection Resonance and Its Connection to the Stability of Outer Satellites

Tadashi Yokoyama,[1] Ernesto Vieira Neto,[2] Othon Cabo Winter,[2] Diogo Merguizo Sanchez,[1] and Pedro Ivo de Oliveira Brasil[1]

[1] *Departamento de Estatística, Matemática Aplicada e Computação (DEMAC),*
 Instituto de Geociências e Ciências Exatas (IGCE), Universidade Estadual Paulista (UNESP),
 Caixa Postal 178, 13500-970 Rio Claro, SP, Brazil
[2] *Grupo de Dinâmica Orbital e Planetologia, Faculdade de Engenharia de Guaratinguetá (FEG),*
 Universidade Estadual Paulista (UNESP), Campus de Guaratinguetá, Caixa Postal 205,
 CEP 12516-410 Guaratinguetá, SP, Brazil

Correspondence should be addressed to Tadashi Yokoyama, tadashi@ms.rc.unesp.br

In terms of stability around the primary, it is widely known that the semimajor axis of the retrograde satellites is much larger than the corresponding semimajor axis of the prograde satellites. Usually this conclusion is obtained numerically, since precise analytical derivation is far from being easy, especially, in the case of two or more disturbers. Following the seminal idea that what is unstable in the restricted three-body problem is also unstable in the general N-body problem, we present a simplified model which allows us to derive interesting resonant configurations. These configurations are responsible for cumulative perturbations which can give birth to strong instability that may cause the ejection of the satellite. Then we obtain, analytically, approximate bounds of the stability of prograde and retrograde satellites. Although we recover quite well previous results of other authors, we comment very briefly some weakness of these bounds.

1. Introduction

Among the puzzling questions in the solar system inventory, the problem of the irregular moons of the Jovian planets is a crucial challenge and controversial topic. Their orbits are highly tilted, very eccentric, and in opposition to inner satellites; these moons orbit the mother planets at very large distances, being strongly disturbed by the Sun. Recently, the number of these distant moons has increased at least one order of magnitude than the pre-CCD era (Sheppard et al. [1], Holman et al. [2], and references therein). These discoveries have provided a lot of new ingredients indicating interesting clues to understand the origin, composition,
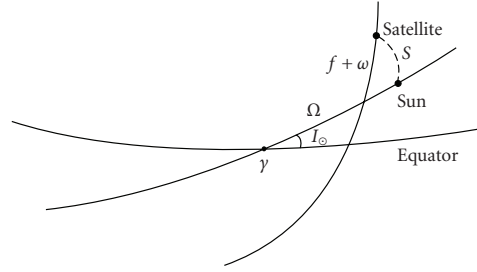
Figure 1: Geometry of the problem.

and evolution of such objects. In this work we basically analyze some dynamical aspects which govern the escape process of an irregular satellite. It is well known that there are some remarkable differences in the stability domain between retrograde and prograde moons (Alvarellos and Dones [3], Hamilton and Krivov [4], Vieira Neto et al. [5, 6], Ćuk and Gladman [7], Domingos et al. [8], etc.). Recently, a large number (about 60000) of irregular satellites were numerically integrated by Nesvorný et al. [9]. Among some interesting new results, they also confirm the role played by the Kozai-Lidov and evection resonances which in general provoke the escape of these objects. The evection resonance is caused by the 1 : 1 commensurability between ϖ (longitude of the satellite pericenter) and $\lambda_{\odot}$ (Sun's mean longitude) where index $\odot$ refers to the Sun's elements. Nesvorný et al. [9] show that once a prograde satellite is in an evection resonance, the critical angle $\varpi - \lambda_{\odot}$ can librate around $180°$, resulting in a cumulative perturbation which can cause the escape of the satellite. For the retrograde satellites, the phenomenon is similar, however the definition of the critical angle must be changed and the libration center is $90°$ or $270°$. Nesvorný et al. [9] show that both resonances occur in the vicinity of some fixed values of the semimajor axes of the satellite. Some investigations on these values were done by Alvarellos and Dones [3] and Hamilton and Krivov [4], using some concepts of Jacob constant and generalization of the Tisserand constant for the restricted three-body problem. In this work we derive an alternative and simple way to obtain, theoretically, these semimajor values. Through the steps we outline here, it becomes very clear the main idea which associates the libration of the critical angle with the appearance of the instability.

2. Disturbing function: second-order expansion

Let us assume a Cartesian system fixed on Jupiter. Initially, the reference plane is the equator of the planet. Figure 1 shows the geometry of the problem. The disturbing function for the motion of a satellite perturbed by the Sun is

$$R_{\odot} = \frac{k^2 M_{\odot} r^2}{2 r_{\odot}^3} \left(3 \cos^2(S) - 1\right), \tag{2.1}$$

where third-order terms in the ratio of the distances $(r/r_{\odot})$ are neglected; k^2 is the constant of the gravitation, $M_{\odot}$ is the mass of the Sun, and r and $r_{\odot}$ are the position vector of the satellite and of the Sun, respectively. S is the angular distance between Sun and the satellite. From the geometry we have

$$\cos(S) = \frac{x}{r} \frac{x_{\odot}}{r_{\odot}} + \frac{y}{r} \frac{y_{\odot}}{r_{\odot}} + \frac{z}{r} \frac{z_{\odot}}{r_{\odot}}. \tag{2.2}$$

We adopt the classical notations: $(a, e, I, l, \omega, \Omega, f)$ stand for semimajor axis, eccentricity, inclination, mean anomaly, argument of pericenter, longitude of the node, and true anomaly, respectively, for the elements of the satellite. The same variables with the index $\odot$ are used for the Sun.

Now let us choose the Sun-Jupiter orbital plane as the reference plane, so that $z_\odot = I_\odot = 0$ and

$$\cos(S) = \left[\cos(f + \omega)\cos(\Omega) - \sin(f + \omega)\sin(\Omega)\cos(I)\right]\left[\cos(f_\odot + \varpi_\odot)\right]$$
$$+ \left[\cos(f + \omega)\sin(\Omega) + \sin(f + \omega)\cos(\Omega)\cos(I)\right]\left[\sin(f_\odot + \varpi_\odot)\right], \quad (2.3)$$
$$\cos(S) = \cos(\theta_1)\cos(\theta_2) + \sin(\theta_1)\sin(\theta_2)\cos(I),$$

where $\theta_1 = f + \varpi$, $\theta_2 = f_\odot + \varpi_\odot - \Omega$ (ϖ, $\varpi_\odot$ are the longitudes of pericenter of satellite and of the Sun, resp.).

Therefore we have

$$R_\odot = \frac{k^2 M_\odot a^2}{2r_\odot^3} \frac{r^2}{a^2} \left\{ -\frac{1}{4} + \frac{3}{4}\left[\cos(2\theta_2) + \cos(2\theta_2)\cos(2\theta_1) + \cos(2\theta_1)\right] + \frac{3}{4}\cos^2(I) \right.$$
$$\left. \times \left[1 - \cos(2\theta_2) - \cos(2\theta_1) + \cos(2\theta_2)\cos(2\theta_1)\right] + \frac{3}{2}\cos(I)\sin(2\theta_1)\sin(2\theta_2) \right\}.$$
$$(2.4)$$

Note that terms like r^2/a^2, $(r^2/a^2)\cos(2f)$, $(r^2/a^2)\sin(2f)$, and so forth can be averaged through simple formulae of the classical two-body problem (Yokoyama et al. [10]). Let $\langle \cdot \rangle$ indicates average with respect to the mean anomaly of the satellite:

$$\left\langle \frac{r^2}{a^2} \right\rangle = \frac{1}{2\pi} \int_0^{2\pi} \frac{r^2}{a^2} dl. \quad (2.5)$$

Omitting the details, we easily get

$$\left\langle \frac{r^2}{a^2} \right\rangle = 1 + \frac{3}{2}e^2, \qquad \left\langle \frac{r^2}{a^2}\cos(2f) \right\rangle = \frac{5}{2}e^2, \qquad \left\langle \frac{r^2}{a^2}\sin(2f) \right\rangle = 0. \quad (2.6)$$

Note that up to now, in the above calculations neither expansion in eccentricity nor in inclination was used. This is an important point since we have to deal with high values of the eccentricity and inclination. The expression of the averaged disturbing function up to second order in the ratio r/a is

$$R_\odot = \frac{k^2 M_\odot a^2}{2r_\odot^3} \left\{ -\frac{1}{4}\left(1 + \frac{3}{2}e^2\right) \right.$$
$$+ \frac{3}{4}\left[\left(1 + \frac{3}{2}e^2\right)\cos(2\theta_2) + \frac{5}{2}e^2\cos(2\varpi - 2\Omega)\cos(2\theta_2) + \frac{5}{2}e^2\cos(2\varpi - 2\Omega)\right]$$
$$+ \frac{3}{4}\cos^2(I)\left[\left(1 + \frac{3}{2}e^2\right) - \left(1 + \frac{3}{2}e^2\right)\cos(2\theta_2)\right.$$
$$\left. -\frac{5}{2}e^2\cos(2\varpi - 2\Omega) + \frac{5}{2}e^2\cos(2\varpi - 2\Omega)\cos(2\theta_2)\right]$$
$$\left. + \frac{15}{4}e^2\sin(2\varpi - 2\Omega)\sin(2\theta_2)\cos(I) \right\}.$$
$$(2.7)$$

(a)

(b)
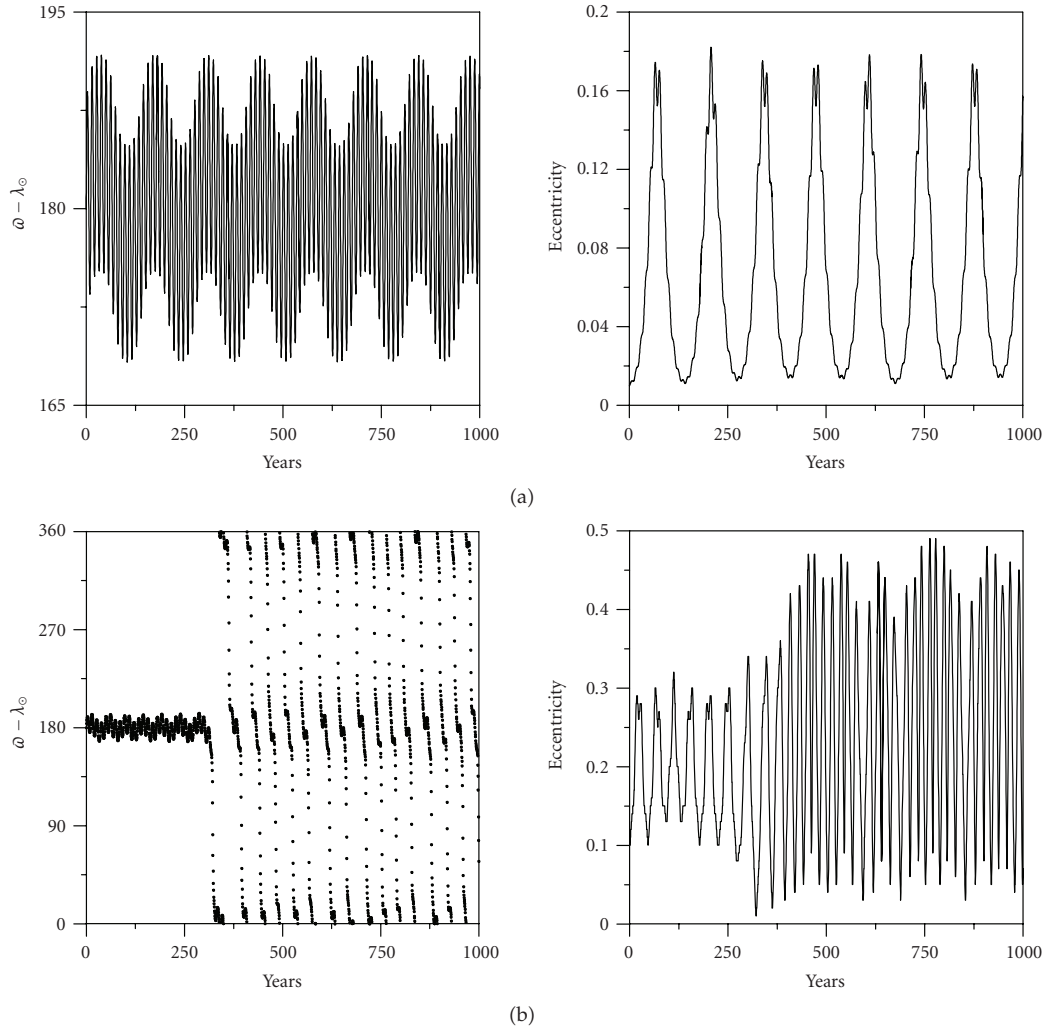
Figure 2: (a) Prograde satellite. Initial conditions: $a = 395R_J$, $e = 0.01$, $I = 1.5°$, and $\varpi = 180°$. (b) Prograde satellite. Initial conditions: $a = 400R_J$, $e = 0.1$, $I = 1°$ and $\varpi = 180°$.

3. Prograde satellites

Considering this disturbing function, we integrate the Lagrange variational equations (Danby [11]). Figure 2(a) shows the behavior of the critical angle ($\varpi - \lambda_\odot$) and the eccentricity. Note that if the libration of this angle is centered at 180°, the apocenter of the satellite will always be close to Sun. In Figure 3 we show this situation which is a critical case when Jupiter, Sun, and apocenter are aligned, that is, the amplitude of the libration is zero.

In this case, no matter the period of the satellite, each time it passes through the apocenter S we have the Sun, satellite, and Jupiter aligned with the first two in their closest approach.

Therefore, it will occur a cumulative perturbation. In particular, note that this is the worst situation for the orbital stability of a massless object. Now suppose that this configuration
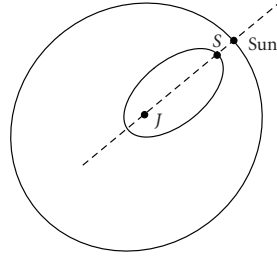
Figure 3: Prograde case: $\varpi - \lambda_\odot = 180°$.

occurs repeatedly. After some passages, certainly, the eccentricity and the semimajor axis of the satellite will be strongly disturbed. They should increase approaching to some dangerous limit. This is clearly shown in Figure 2(b). Note, however, that while $\varpi - \lambda_\odot$ remains in libration, the eccentricity is not so high (~0.3). The significant increase of the eccentricity appears only when $\varpi - \lambda_\odot$ enters in a circulation regime. This dynamics will be discussed in Section 5. Of course in this model since we are using averaged equations, by definition, the semimajor axis is kept constant. Therefore, within the limits of our model the escape does not necessarily occur during this short integration time. The initial conditions we used were $a = 400R_J(0.538R^H)$, $e = 0.1$, $I = 1°$, $\varpi - \lambda_\odot = 180°$, $\varpi = 180°$, $a_\odot = 5.202603$ AU, $e_\odot = 0.048497$, $\omega_\odot = 0°$, and $\Omega_\odot = 0°$ (R_J means Jupiter's equatorial radius and R^H is Hill's radius).

Once we have this basic information we can go further and confirm very easily; some results shown in Hamilton and Krivov [4]. Since we have shown that the appearance of the evection resonance causes large variation of the eccentricity, we assume that the corresponding semimajor axis of the evection resonance has to do with the limit of stability of the satellite around the planet. Therefore, we take this statement for granted and search the value of the semimajor axis. To this end, in the averaged disturbing function (2.7), let us consider only the secular and resonant terms due to the evection. All other remaining terms can be neglected. In particular, since we showed a libration in $\varpi - \lambda_\odot = 180°$, we fix this angle at $180°$. Again, from Lagrange's equation we easily obtain

$$\dot{\varpi} \cong \frac{k^2 M_\odot (1 - e^2)^{1/2}}{2na_\odot^3} \left\{ \frac{9}{8} + \frac{33}{8}\cos^2(I) + \frac{15}{4}\cos I \right\} + o\left(\sin(I)\right). \tag{3.1}$$

Now, if we consider $I = e = 0$, we have

$$\dot{\varpi} \cong \frac{9}{2}\frac{k^2 M_\odot}{na_\odot^3}. \tag{3.2}$$

Since the apparent motion of the Sun is Keplerian, we take $n_\odot = \sqrt{k^2(M_\odot + m_J)/a_\odot^3}$.

Hill's radius is defined as $R^H = a_\odot(m_J/3M_\odot)^{1/3}$.

Therefore, equating $\dot{\varpi} = n_\odot$, we get the resonant value of the semimajor axis:

$$a^* = 0.529R^H, \tag{3.3}$$

which is in quite agreement with Hamilton and Krivov [4] and the numerical results of Nesvorný et al. [9].

Recall that the semimajor axes we used in Figures 2(a), 2(b) were $a = 0.531R^H(395R_J)$ and $a = 0.538R^H(400R_J)$, respectively.

A simple inspection in (2.7) shows that critical angle always appears in the form $2(\varpi - \lambda_\odot)$. This sugests that $\varpi - \lambda_\odot = 0$ is also another center of libration.

We can confirm this very easily. Selecting only secular and resonant terms in (2.7) we have

$$R_\odot = \frac{k^2 M_\odot a^2}{2a_\odot^3}\left\{\frac{1}{2}\left(1 + \frac{3}{2}e^2\right) + \frac{15}{4}e^2\cos(2\varpi - 2\lambda_\odot)\right\}, \qquad (3.4)$$

where we assumed Jupiter in a circular motion and $I = 0$.

The conservative Hamiltonian can easily be derived from the above simplified relation:

$$H = \frac{k^2 M_\odot a^2}{2a_\odot^3}\left\{\frac{3}{4}e^2 + \frac{15}{4}e^2\cos(2\varpi - 2\lambda_\odot)\right\} - n_\odot L_\odot, \qquad (3.5)$$

where $L_\odot$ is the canonical momentum conjugated to $\lambda_\odot$. Considering the classical Delaunay canonical variables: ϖ, $G - L$ (Brouwer and Clemence [12]), and writing e^2 in terms of G and L, we proceed with a new trivial canonical transformation:

$$(\varpi, \lambda_\odot, G - L, L_\odot) \longrightarrow (\alpha_1, \alpha_2, P_1, P_2), \qquad (3.6)$$

where $\alpha_1 = \varpi - \lambda_\odot$, $P_1 = G - L$, $\alpha_2 = \lambda_\odot$, $P_2 = L_\odot + (G - L)$.

This allow us to write a one-degree-of-freedom problem, since α_2 becomes a kinosthenic variable;

$$H = \frac{k^2 M_\odot a^2}{2a_\odot^3}\left\{\frac{3}{4}e^2 + \frac{15}{4}e^2\cos(2\alpha_1)\right\} + n_\odot G, \qquad (3.7)$$

where $e^2 = (L^2 - (P_1 + L)^2)/L^2$. Note that with a completely different way, we obtained (3.4) of Hamilton and Krivov [4].

The level curves of the above Hamiltonian confirm that both $\varpi - \lambda_\odot = 0°$ and $180°$ are stable equilibrium points of the system. In Figure 4 we show the level curves in the plane $e\cos(\varpi - \lambda_\odot)$, $e\sin(\varpi - \lambda_\odot)$. This clearly shows that the longitude of the pericenter of the satellite can remain stably pointing to Sun direction or to the opposite direction. Of course the net effect of this dynamics is to stretch the satellite orbit toward and away from the Sun (Figure 4). We also can say that the $\varpi - \lambda_\odot = 180°$ is a critical configuration, so that we expect to have escape of the satellite mostly in this situation, not when $\varpi - \lambda_\odot = 0°$. In Sections 5, 6 we confirm numerically that escapes occur following these kind of behavior.

These mentioned two centers of libration play important role as we can see in Section 6.

4. Retrograde satellites

For the retrograde satellites, the definition of the longitude of the pericenter should be changed (Saha and Tremaine [13]). Let ϖ_I be the longitude of the pericenter for this case. Therefore, we have

$$\varpi_I = \Omega - \omega. \qquad (4.1)$$
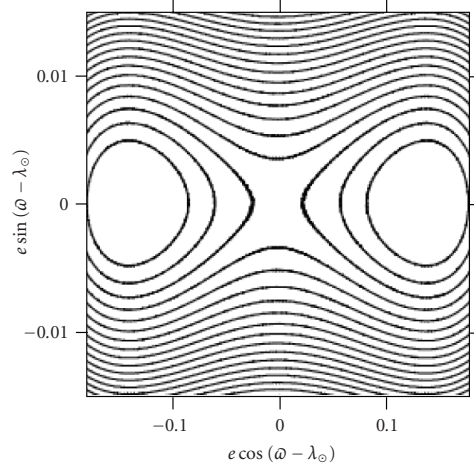
Figure 4: Level curves of Hamiltonian (3.7) with $a = 396R_J$.

Let ϖ be the usual longitude of the prograde case. Then, with a simple algebra we can relate both:

$$\varpi_I = 2\Omega - \varpi. \tag{4.2}$$

As in the previous case, we integrate again Lagrange's equations taking the disturbing function given by (2.7).

In the precedent figures, we considered the following initial condictions: $\omega = 0°$, $\Omega = 90°$ (Figure 5(a)), and $\omega = 90°$, $\Omega = 0°$ (Figure 5(b)). For Jupiter (Sun) we adopted $a_\odot = 5.202603$ AU, $e_\odot = 0.048497$, $\omega_\odot = 0°$, $\Omega_\odot = 0°$, and $l_\odot = 0°$.

This time we see that the critical angle $\varpi_I - \lambda_\odot$ librates around $90°$ or $270°$. The situation is not so drastic as in the direct case. The schematic geometry given in Figure 6 repeats each time the satellite passes through S.

From Lagrange's variational equations we have

$$\dot{\Omega} = \frac{3}{2}\frac{G_C}{na^2}, \qquad \dot{\varpi} = \frac{9}{2}\frac{G_C}{na}, \tag{4.3}$$

where $G_C = k^2 M_\odot a^2 / 2a_\odot^3$. As before we fixed some values considering the current resonance: $\Omega - \omega - \lambda_\odot = 90°$, $I = 180°$, and $e = 0$. Again equating: $\dot{\varpi}_I = n_\odot$, we get: $a^* = 0.6933R^H$ ($\approx 515.3R_J$) which coincides again with the results given in Hamilton and Krivov [4].

Recall that the semimajor axis we used in Figures 5(a) and 5(b) was $a = 0.7R^H$ ($520R_J$). It is worth noting that compared to the previous direct case; the present resonance is not very strong since the closest approach with the Sun is not like in the direct case. Even so, the cumulative effect works quite efficiently in driving the eccentricity and semimajor axis to critical values, sometimes causing ejection of the satellite. This is clear in Figure 5(b).

Again following the same steps outlined for the prograde case, the conservative Hamiltonian can be written as

$$H = \frac{k^2 M_\odot a^2}{2a_\odot^3}\left\{\frac{3}{4}\left(1 - \frac{P_1^2}{L^2}\right) + \frac{15}{4}\left(1 - \frac{P_1^2}{L^2}\right)\cos(2\sigma_1)\right\} - n_\odot P_1, \tag{4.4}$$

(a)

(b)
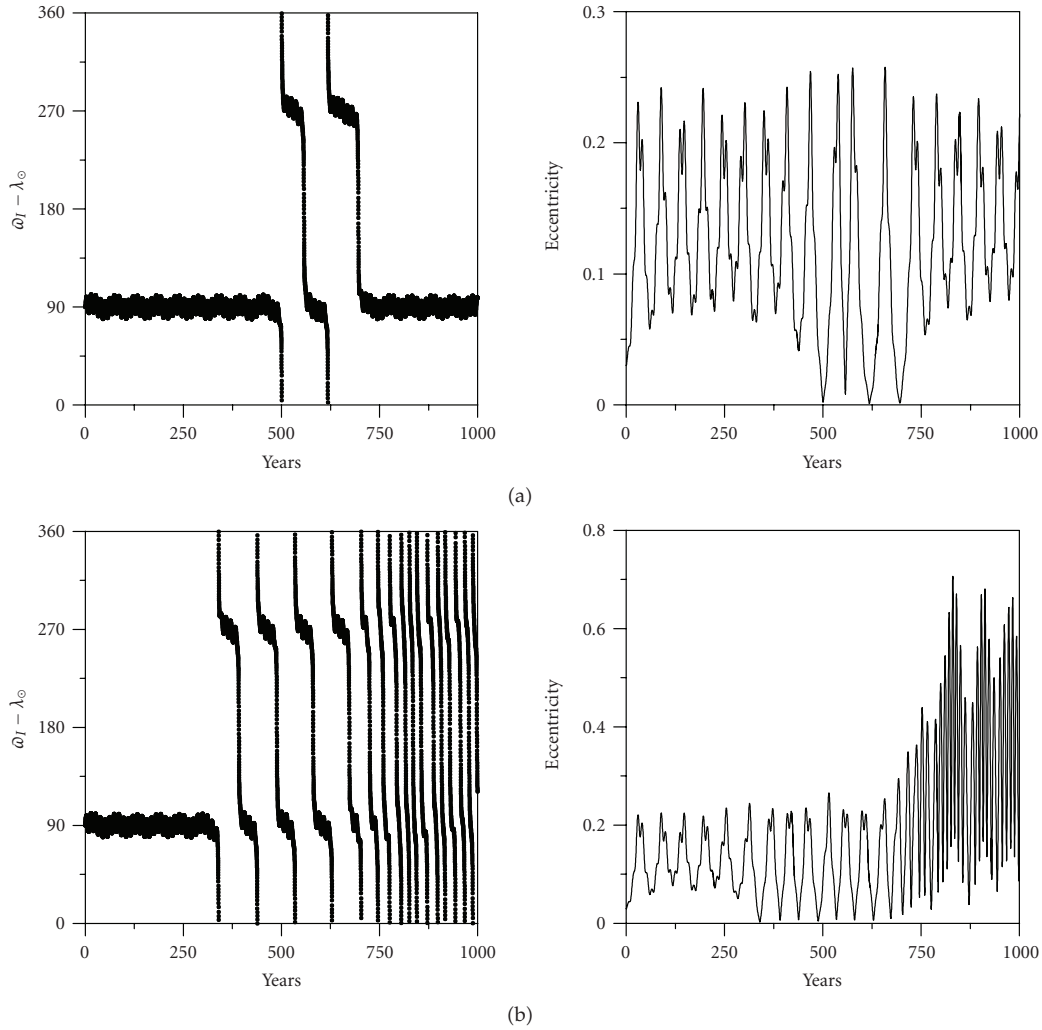
Figure 5: (a) Retrograde satellite. Initial conditions: $a = 520R_J$, $e = 0.03$, $I = 176°$, $\omega = 0°$, and $\Omega = 90°$. (b) Retrograde satellite. Initial conditions: $a = 520R_J$, $e = 0.03$, $I = 176°$, $\omega = 90°$, and $\Omega = 0°$.

where P_1 and σ_1 are the canonical conjugated variables defined by $P_1 = G = L(1 - e^2)^{1/2}$ and $\sigma_1 = \varpi_I - \lambda_\odot$.

Drawing level curves for $H(P_1, \sigma_1)$, we can easily check that $\sigma_1 = 90°$, $270°$ are stable equilibrium solutions (Figure 7). This time, in this approximation, the tendency of the orbits is to elongate perpendicularly to the Sun-satellite direction, as suggested in Figure 6.

5. Numerical tests with exact equations

In this section we show some simulations considering the exact differential equations of a satellite of Jupiter disturbed by the Sun. In terms of the radius of the planet, the resonant semimajor axis for the prograde case is $a^* = 393R_J$. Time variations of the eccentricity and
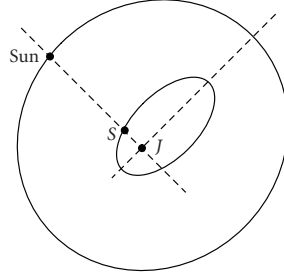
Figure 6: Retrograde case: $\varpi_I - \lambda_\odot = 90°$.
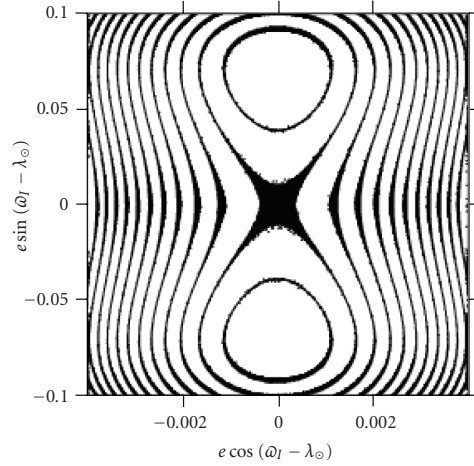
Figure 7: Level curves of Hamiltonian (4.4) with $a = 516.4R_J$.

$\varpi - \lambda_\odot$ are shown in Figure 8. The initial conditions were $a = 355R_J$, $e = 0.001$, $I = 1°$, $\omega = 180°$, and $\Omega = 0°$. Initially, the critical angle remains librating around zero when the eccentricity remains almost bounded and less than 0.4.

In Figure 9 we consider $a = 355R_J$, $e = 0.011$, $I = 1°$, $\omega = 180°$, and $\Omega = 0°$. As before, initially, libration is around $0°$ and in the beginning the dynamics is very similar to the previous figure. A significant increase of the eccentricity is observed when $\varpi - \lambda_\odot$ enters in the circulation regime and escape occurs at about $t \approx 140$ years.

Figure 10 shows a case when the libration is centered only in $180°$. As before, the increase and escape occur when $\varpi - \lambda_\odot$ changes to a circulation regime.

Figure 4 is very useful to interpret the results of the previous simulations. Usually the region deep inside the libration (near the center) is very regular and is related to the existence of stable periodic orbits. For this reason, if $\varpi - \lambda_\odot$ is trapped inside a libration region, the eccentricity remains bounded, without suffering large excursions. On the other hand, circulation regime allows large excursions of the eccentricity.

That said, we can analyze the dynamics of the three previous figures. In Figure 8, initially, the satellite librates around $\varpi - \lambda_\odot = 0°$ up to about 35 years when a short transition to circulation appears for $t \sim 40$ years, but soon, the system again goes back to original libration regime up to about $t \sim 75$ years when the libration center moves to $180°$ at $t \sim 80$ years. Next,
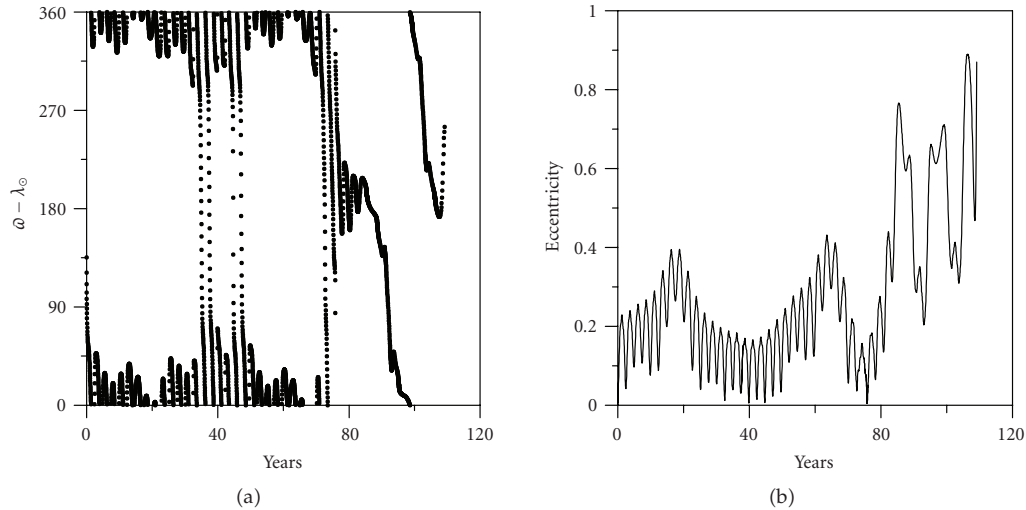
(a)   (b)

Figure 8: Prograde satellite. Initial conditions: $a = 355R_J$, $e = 0.001$, $I = 1°$, $\omega = 180°$, and $\Omega = 0°$.
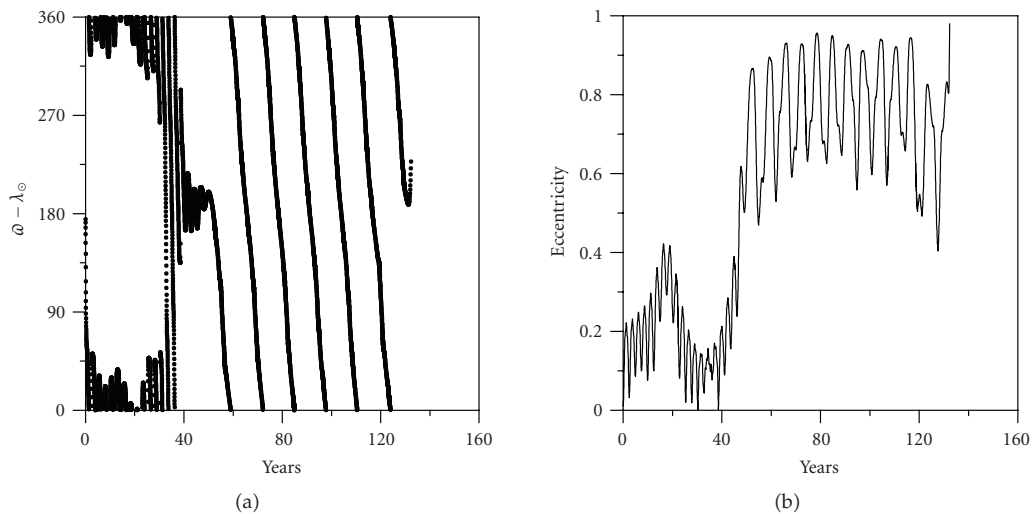

(a)   (b)

Figure 9: Prograde satellite. Initial conditions: $a = 355R_J$, $e = 0.011$, $I = 1°$, $\omega = 180°$, and $\Omega = 0°$.

a circulation appears, so that the motion is no more trapped inside a region of bounded small eccentricity, as discussed above. Outside of the libration curves the motion can experience, very easily, higher variations mostly because now the complete problem is not integrable and the domain of the regular region of the level curves of Figure 4, certainly is very reduced (modified). Indeed, numerical examples indicate that the librations of $\varpi - \lambda_\odot$, in general, are not permanent and the perturbations always cause transitions to circulation. In Figure 8, the eccentricity remains below 0.4 and escape occurs only after the resonant angle changes to circulation regime. The jump of the eccentricity when $\varpi - \lambda_\odot$ changes to circulation is best illustrated in Figure 9. In Figure 10 the libration is always centered in 180°, but even so, there

(a)

(b)
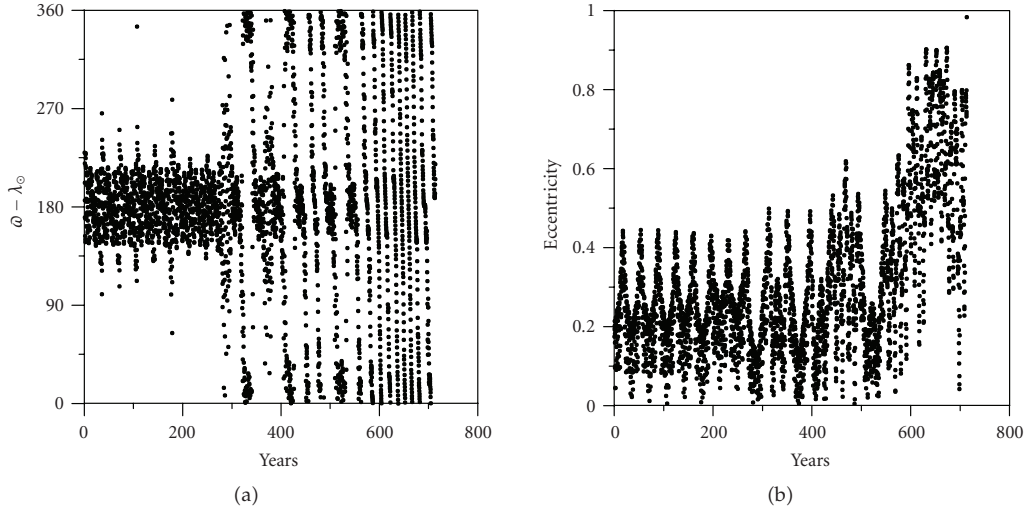
Figure 10: Prograde satellite. Initial conditions: $a = 344.088R_J$, $e = 0.001$, $I = 1°$, and $\omega = \Omega = 0°$.

are some brief transitions when $\varpi - \lambda_\odot$ attains $0°$ or $360°$. Again, as predicted, the escape occurs after circulation appears. Although it is not clear in these figures, we have checked that the escapes always occur in the neighborhood of $\varpi - \lambda_\odot = 180°$.

As pointed out in Hamilton and Krivov, the limit $a = 393R_J$ for the resonant semimajor axis is rather overestimated. In some cases, escapes can occur for $a = 345R_J$. One of the reasons of this discrepancy is the fact that our simplified model in (2.1) considers Jupiter in circular orbit, however in the numerical simulations Jupiter's eccentricity is $e_J = 0.048497$. Another point which is important is related to the expansion of the function given in (2.7), where terms of higher order in the ratio $(r/r_\odot)$ were neglected. The inclusion of higher order terms is not difficult but laborious. We intend to investigate in a future work.

Our numerical simulations also show that sometimes the initial value of the pericenter plays an important role in the stability. This seems to be more salient for values not so close to $a = a^*$. For instance, in the case of $a = 350$ we found stability if $\omega = 180°$, while if $\omega = 0$ the satellite is ejected in less than 1000 years.

For the retrograde case we have $a^* = 515.31R_J$. Figures 11 and 12 show two examples of escape, where the center of libration changes several times, much more often than in the prograde case. From Figure 6 we see that the two centers of libration are completely symmetric in opposition to the centers of the prograde case (Figure 3). Therefore, the behavior of the eccentricity around these two centers is similar. As before, the change of the center of the libration ($90°$ to $270°$ and vice versa) is predicted in the complete problem, due to the nonintegrability. Figure 7 suggests that the occurrence of these changes is related to a chaotic motion in the neighborhood of a separatrix. Again, each time the critical angle circulates, the trajectory is in a region, where large excursions in eccentricity should occur. Therefore sooner or latter this can result in an escape.

Indeed in Figures 11-12, after several changes of the center of the libration, escape ocurs and in both cases we confirmed again the remarkable feature we always have observed, that is,
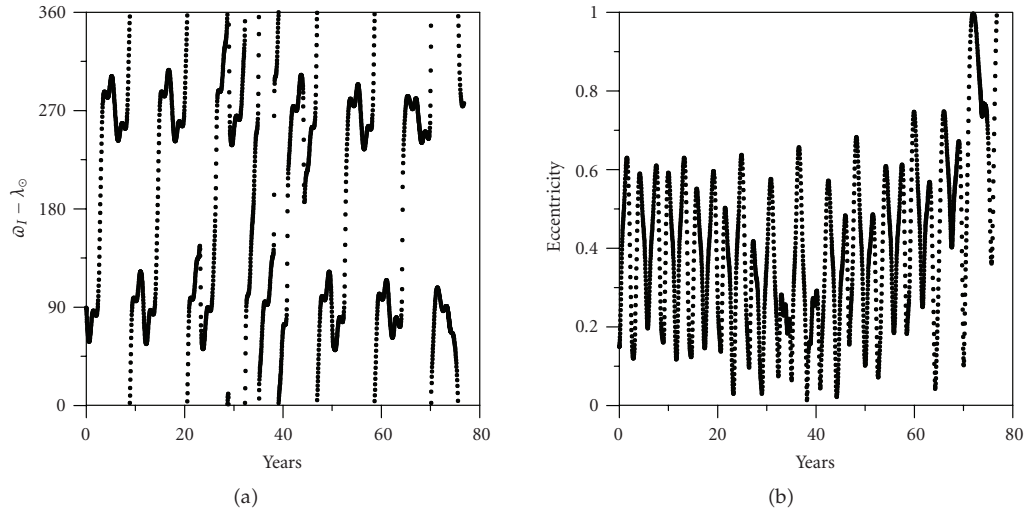
(a)

(b)

Figure 11: Retrograde satellite. Initial conditions: $a = 528.4R_J$, $e = 0.15$, $I = 179°$, $\omega = 90°$, and $\Omega = 180°$.
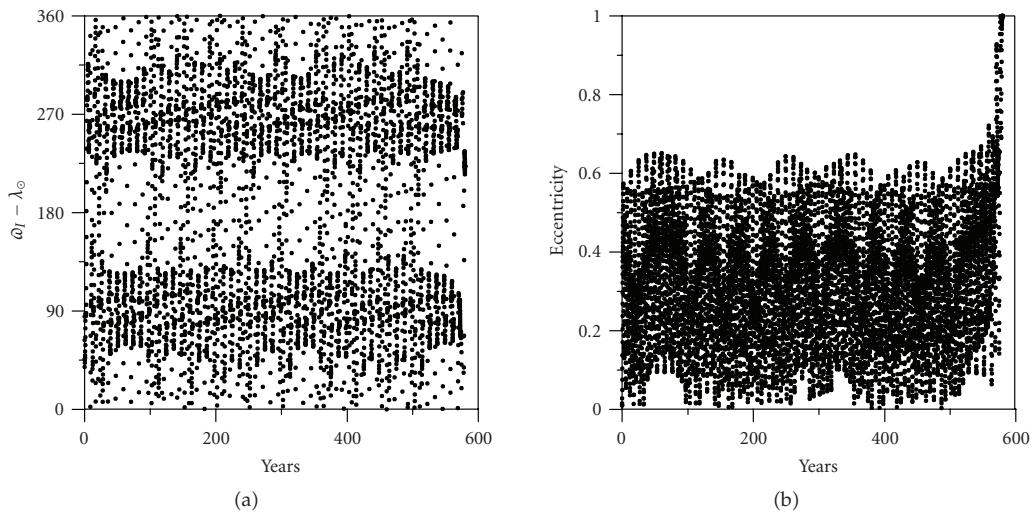

(a)

(b)

Figure 12: Retrograde satellite. Initial conditions: $a = 516.8888R_J$, $e = 0.01$, $I = 179°$, $\omega = 90°$, and $\Omega = 180°$.

in general, escapes occur in the vicinity of the center of the libration ($\varpi - \lambda_\odot = 180°$ for prograde satellites and $\varpi_I - \lambda_\odot = 90°$ or $270°$ for retrograde case).

6. Some islands of stability

As mentioned before, the bounds $395R_J$ and $515R_J$ are approximate and overestimated. Certainly, a model using higher order expansion of the disturbing function $R_\odot$ would provide better determination of these values. Since expansion in Legendre polynomials is crucial for large values of the ratio of the distances, no wonder about some discrepancies in these numbers
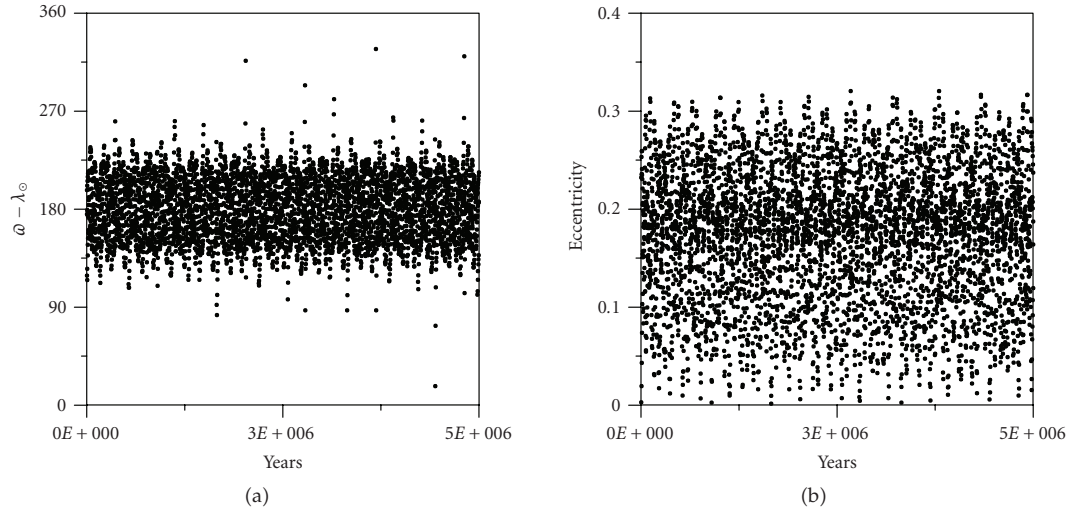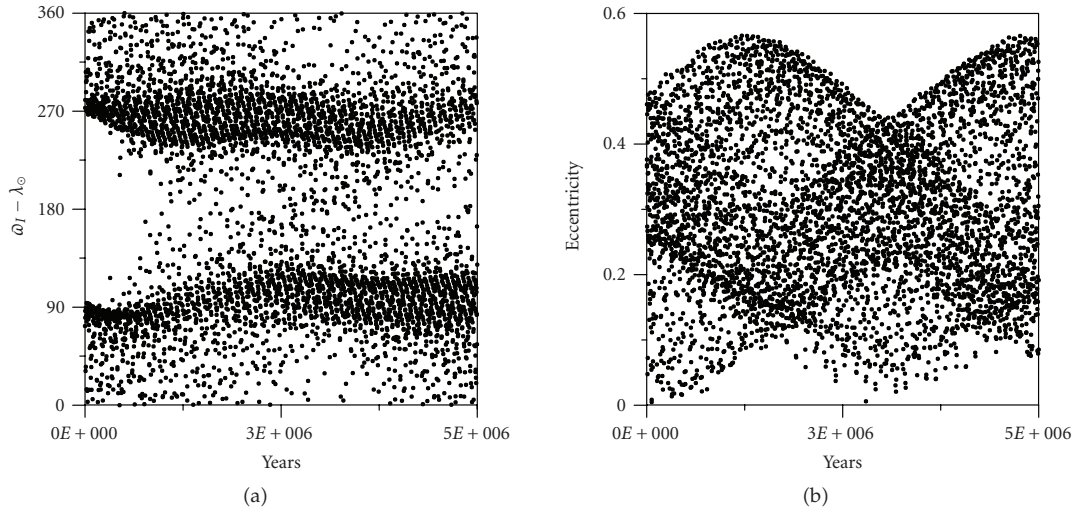
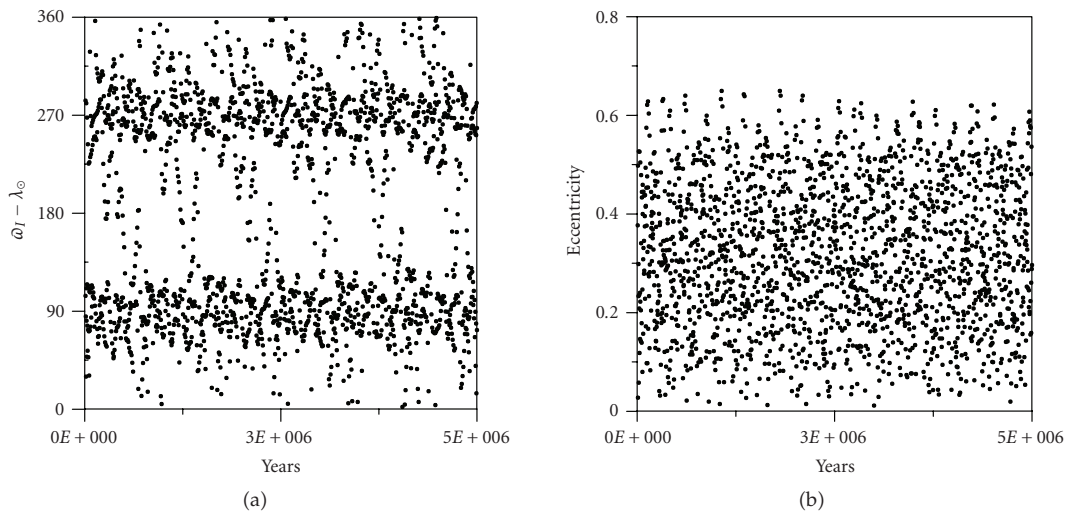**Figure 13:** Prograde satellite. Initial conditions: $a = 340R_J$, $e = 0.001$, $I = 1°$, $\omega = 0°$, and $\Omega = 0°$.
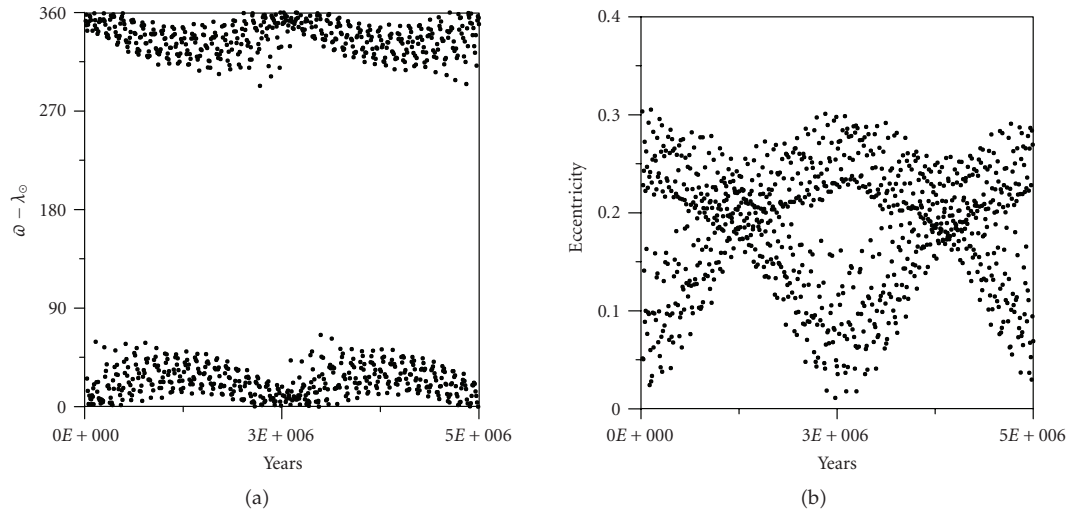
Figure 14: Prograde satellite. Initial conditions: $a = 352R_J$, $e = 0.001$, $I = 1°$, $\omega = 180°$, and $\Omega = 0°$.

since they were obtained taking the simplest expansion of second order in (3.1). However, no matter the improvement in this determination, we show, in this section, the existence of several islands of stability beyond the values mentioned above.

In Figures 4 and 7 we found two stable equilibrium centers. Although the onset of the resonance can cause large variations and sometimes escape, however if the satellite is trapped deep inside the libration curve, this orbit can remain very stable, free of dangerous variations in eccentricity. In general these are periodic (quasi-) stable orbits and are not isolated. Our numerical experiments have shown that there are some finite intervals of the semimajor axis

(a)

(b)

Figure 15: Retrograde satellite. Initial conditions: $a = 583R_J$, $e = 0.001$, $I = 179°$, $\omega = 0°$, and $\Omega = 0°$.

(a)

(b)

Figure 16: Retrograde satellite. Initial conditions: $a = 612R_J$, $e = 0.001$, $I = 179°$, $\omega = 180°$, and $\Omega = 0°$.

even for $a > 395R_J$, where the satellite survives for at least 5 myr. Figures 13 and 14 show typical examples, where the satellite remains trapped in $\varpi - \lambda_\odot = 0°$ and 180°, respectively.

In the case of retrograde orbits we found much more interesting intervals of stability. We show only two Figures 15 and 16, where although the resonant angle changes sometimes from 90° to 270°, the eccentricity remains quite safe from collision or escapes. Note that in these two figures, the semimajor axis is much larger than a^*. Recall that this kind of stable regions is possible thanks to the two stable libration centers predicted in our simplified model. In other words, the appearance of the two stable centers is related to the existence of a family of stable periodic orbits. In the complete problem, part of this region of stability is still preserved.

Therefore, we can numerically find some of these orbits even for high distances. Finally, we list some semimajor axis intervals ($a > a^*$), where stability was found for at least 5 million years, as follows:

$$[604\text{–}640]\ (l = 180°,\ \omega = l_\odot = 0°);$$

$$[600\text{–}642]\ (l = l_\odot = 0°,\ \omega = 180°);$$

$$[564\text{–}676]\ (l = l_\odot = \omega = 180°);$$

$$[568\text{–}677]\ (l = \omega = 0°,\ l_\odot = 180°);$$

$$[576\text{–}620],\ [652\text{–}680]\ (l = 0°,\ \omega = l_\odot = 180°);$$

$$[572, 618],\ [654\text{–}682]\ (l = l_\odot = 180°,\ \omega = 0°);$$

where within parentesis, on the right of the intervals, we indicate the initial values for l, $l_\odot$, and ω. For the remaining values we considered $e = 0.001$, $I = 179°$, and $\Omega = \Omega_\odot = 0°$. Most probably some of these orbits are the same as pointed out by Winter [14] for the Earth-Moon problem.

7. Conclusion

We have derived, analytically, the values of the semimajor axis, where evection resonances can occur. These values are important, since they define approximated limits, where direct and retrograde orbits can remain stable around a planet. Through a simple model based on the restricted three-body problem these values were obtained and checked against exact numerical integration. Using a completely different way, we confirm previous results of other authors. Our methodology is based on the classical expansion of the disturbing function which can be improved much more if we consider higher order terms. Therefore, we think that the current values: $395R_J$ and $515R_J$ perhaps can be improved. We also showed that the existence of stable orbits beyond the above values is related to the stability of the region in the vicinity of the libration centers of the evection resonance, which still persist even for large values of the semimajor axis.

Acknowledgments

References

[1] S. S. Sheppard, D. Jewitt, and J. Kleyna, "An ultradeep survey for irregular satellites of Uranus: limits to completeness," *The Astronomical Journal*, vol. 129, no. 1, pp. 518–525, 2005.

[2] M. J. Holman, J. J. Kavelaars, T. Grav, et al., "Discovery of five irregular moons of Neptune," *Nature*, vol. 430, no. 7002, pp. 865–867, 2004.

[3] J. L. Alvarellos Jr. and L. Dones, "Orbital stability of hypothetical distant satellites of the Jovian planets," *Bulletin of the American Astronomical Society*, vol. 28, no. 3, p. 1185, 1996.

[4] D. P. Hamilton and A. V. Krivov, "Dynamics of distant moons of asteroids," *Icarus*, vol. 128, no. 1, pp. 241–249, 1997.

[5] E. Vieira Neto, O. C. Winter, and T. Yokoyama, "The effect of Jupiter's mass growth on satellite capture. Retrograde case," *Astronomy & Astrophysics*, vol. 414, no. 2, pp. 727–734, 2004.

[6] E. Vieira Neto, O. C. Winter, and T. Yokoyama, "Effect of Jupiter's mass growth on satellite capture. The prograde case," *Astronomy & Astrophysics*, vol. 452, no. 3, pp. 1091–1097, 2006.

[7] M. Ćuk and B. J. Gladman, "Irregular satellite capture during planetary resonance passage," *Icarus*, vol. 183, no. 2, pp. 362–372, 2006.

[8] R. C. Domingos, O. C. Winter, and T. Yokoyama, "Stable satellites around extrasolar giant planets," *Monthly Notices of the Royal Astronomical Society*, vol. 373, no. 3, pp. 1227–1234, 2006.

[9] D. Nesvorný, J. L. A. Alvarellos, L. Dones, and H. F. Levison, "Orbital and collisional evolution of the irregular satellites," *The Astronomical Journal*, vol. 126, no. 1, pp. 398–429, 2003.

[10] T. Yokoyama, M. T. Santos, G. Cardin, and O. C. Winter, "On the orbits of the outer satellites of Jupiter," *Astronomy & Astrophysics*, vol. 401, no. 2, pp. 763–772, 2003.

[11] J. M. A. Danby, *Fundamentals of Celestial Mechanics*, Willmann-Bell, Richmond, Va, USA, 2nd edition, 1992.

[12] D. Brouwer and G. M. Clemence, *Methods of Celestial Mechanics*, Academic Press, New York, NY, USA, 1961.

[13] P. Saha and S. Tremaine, "The orbits of the retrograde Jovian satellites," *Icarus*, vol. 106, no. 2, pp. 549–562, 1993.

[14] O. C. Winter, "The stability evolution of a family of simply periodic lunar orbits," *Planetary and Space Science*, vol. 48, no. 1, pp. 23–28, 2000.

Special Issue on Space Dynamics

Call for Papers

Space dynamics is a very general title that can accommodate a long list of activities. This kind of research started with the study of the motion of the stars and the planets back to the origin of astronomy, and nowadays it has a large list of topics. It is possible to make a division in two main categories: astronomy and astrodynamics. By astronomy, we can relate topics that deal with the motion of the planets, natural satellites, comets, and so forth. Many important topics of research nowadays are related to those subjects. By astrodynamics, we mean topics related to spaceflight dynamics.

It means topics where a satellite, a rocket, or any kind of man-made object is travelling in space governed by the gravitational forces of celestial bodies and/or forces generated by propulsion systems that are available in those objects. Many topics are related to orbit determination, propagation, and orbital maneuvers related to those spacecrafts. Several other topics that are related to this subject are numerical methods, nonlinear dynamics, chaos, and control.

The main objective of this Special Issue is to publish topics that are under study in one of those lines. The idea is to get the most recent researches and published them in a very short time, so we can give a step in order to help scientists and engineers that work in this field to be aware of actual research. All the published papers have to be peer reviewed, but in a fast and accurate way so that the topics are not outdated by the large speed that the information flows nowadays.

Before submission authors should carefully read over the journal's Author Guidelines, which are located at http://www.hindawi.com/journals/mpe/guidelines.html. Prospective authors should submit an electronic copy of their complete manuscript through the journal Manuscript Tracking System at http://mts.hindawi.com/ according to the following timetable:

Manuscript Due	July 1, 2009
First Round of Reviews	October 1, 2009
Publication Date	January 1, 2010

Lead Guest Editor

Antonio F. Bertachini A. Prado, Instituto Nacional de Pesquisas Espaciais (INPE), São José dos Campos, 12227-010 São Paulo, Brazil; prado@dem.inpe.br

Guest Editors

Maria Cecilia Zanardi, São Paulo State University (UNESP), Guaratinguetá, 12516-410 São Paulo, Brazil; cecilia@feg.unesp.br

Tadashi Yokoyama, Universidade Estadual Paulista (UNESP), Rio Claro, 13506-900 São Paulo, Brazil; tadashi@rc.unesp.br

Silvia Maria Giuliatti Winter, São Paulo State University (UNESP), Guaratinguetá, 12516-410 São Paulo, Brazil; silvia@feg.unesp.br